Supplementary information is available in *Nature*'s World-Wide Web site (http://www.nature.com) or as paper copy from the London editorial office of *Nature*.

Acknowledgements

Supported in part by grants from the NIH (A.A., C.B.W. and A.S.) and from the cystic fibrosis foundation (C.B.W. and A.H.). D.M.U. is an Irvington Institute postdoctoral fellow.

Correspondence and requests for materials should be addressed to A.A. (e-mail: aaderem@u.washington.edu).

Table 1 Bone mineral density

Groups	BMD in metaphysis (mg cm^{-3})		BMD in diaphysis (mg cm^{-3})	
	Total	Trabecular	Total	Trabecular
rag1$^{-/-}$	363.3 ± 14.5	309.5 ± 18.5	644.4 ± 3.6	ND
ctla4$^{+/-}$*rag1*$^{-/-}$	379.6 ± 7.3	291.5 ± 15.6	626.4 ± 17.0	462.8 ± 19.6
ctla4$^{-/-}$*rag1*$^{-/-}$	302.7 ± 14.9*	209.5 ± 44.9*	529.8 ± 3.4*	353.0 ± 10.8*

Bone mineral density (BMD) was measured by peripheral quantitative computated tomography of tibial bones from *rag1*$^{-/-}$ ($n = 3$) and *rag1*$^{-/-}$ mice reconstituted with *ctla4*$^{+/-}$ ($n = 3$) or *ctla4*$^{-/-}$ ($n = 3$) bone marrow cells eight weeks after cell transfer.
* Statistically significant difference between different groups (Student's *t*-test: $P < 0.05$). Values are given as the mean ± s.d. ND, not determined.

Nature **402**, 304–309; 1999

Activated T cells regulate bone loss and joint destruction in adjuvant arthritis through osteoprotegerin ligand

Young-Yun Kong*†, Ulrich Feige†‡, Iidiko Sarosi§, Brad Bolon§, Anna Tafuri*, Sean Morony§, Casey Capparelli§, Ji Li‖, Robin Elliott‖, Susan McCabe‖, Thomas Wong¶, Giuseppe Campagnuolo‡, Erika Moran#, Earl R. Bogoch#, Gwyneth Van§, Linh T. Nguyen☆, Pamela S. Ohashi☆, David L. Lacey§, Eleanor Fish¶, William J. Boyle‖ & Josef M. Penninger*☆

** Amgen Institute, 620 University Avenue, Toronto, Ontario M5G 2C1, Canada*
‡ Department of Pharmacology, § Pathology, and ‖ Cell Biology, Amgen Inc., One Amgen Center Drive, Thousand Oaks, California 91320-1789, USA
¶ Department of Medical Genetics & Microbiology, # St Michael's Hospital
☆ Ontario Cancer Institute and the Departments of Medical Biophysics and Immunology, University of Toronto, Toronto, Ontario, Canada
† These authors contributed equally to this work

Bone remodelling and bone loss are controlled by a balance between the tumour necrosis factor family molecule osteoprotegerin ligand (OPGL) and its decoy receptor osteoprotegerin (OPG)[1–3]. In addition, OPGL regulates lymph node organogenesis, lymphocyte development and interactions between T cells and dendritic cells in the immune system[3–5]. The OPGL receptor, RANK, is expressed on chondrocytes, osteoclast precursors and mature osteoclasts[4,6]. OPGL expression in T cells is induced by antigen receptor engagement[7], which suggests that activated T cells may influence bone metabolism through OPGL and RANK. Here we report that activated T cells can directly trigger osteoclastogenesis through OPGL. Systemic activation of T cells *in vivo* leads to an OPGL-mediated increase in osteoclastogenesis and bone loss. In a T-cell-dependent model of rat adjuvant arthritis characterized by severe joint inflammation, bone and cartilage destruction and crippling, blocking of OPGL through osteoprotegerin treatment at the onset of disease prevents bone and cartilage destruction but not inflammation. These results show that both systemic and local T-cell activation can lead to OPGL production and subsequent bone loss, and they provide a novel paradigm for T cells as regulators of bone physiology.

Remodelling of bone involves the synthesis of bone matrix by osteoblasts and bone resorption by osteoclasts[8]. Excessive osteoclast activity is observed in many osteopenic disorders characterized by increased bone resorption and crippling bone damage, including post-menopausal osteoporosis[9], Paget's disease[10] and lytic bone metastases[11]. Local or generalized bone loss has also been reported in chronic infections (hepatitis, HIV)[12], leukaemias[13], autoimmune and allergic diseases[14], and rheumatoid arthritis[15], suggesting that an activated immune system can affect bone physiology. Although cytokines, such as tumour necrosis factor (TNF)α, interleukin (IL)-1, IL-11 and IL-17[16], that regulate immune functions have been implicated in the regulation of bone homeostasis, the molecular mechanism by which the immune system affects bone metabolism has never been established.

Consistent with previous reports[7,17], we observed that OPGL (also known as TRANCE, RANK-L or ODF) messenger RNA expression was upregulated in murine T cells following antigen receptor engagement (Fig. 1a). Specific inhibitor studies showed that induction of OPGL was dependent on protein kinase C (PKC), phosphoinositide 3-kinase (PI3K) and calcineurin-mediated signalling pathways (Fig. 1a). Expression of OPGL protein was detected on the surfaces of activated, but not resting, T cells (Fig. 1b). Activated T cells also secreted soluble OPGL into culture medium (Fig. 1c), and soluble OPGL was detected by enzyme-linked immunosorbent assay (ELISA) (~2.2 ± 0.2 ng ml^{-1} of OPGL in the culture supernatant of CD4$^+$ T cells activated for 4 days with αCD3 plus αCD28). To determine whether the secreted and/or surface forms of OPGL were functionally active, we assessed the ability of both molecules to induce osteoclastogenesis *in vitro*. Haematopoietic bone marrow precursors from wild-type mice were co-cultured with activated CD4$^+$ T cells fixed with paraformaldehyde or with culture supernatants from activated T cells. Both membrane-bound and soluble OPGL supported osteoclast development *in vitro* (Fig. 1d). Osteoclastogenesis was blocked in both cases in the presence of the physiological decoy receptor osteoprotegerin (OPG) (Fig. 1d). As certain T-cell-derived cytokines can regulate OPGL expression in stromal cells, we neutralized many different cytokines including IL-1, TNFα, IL-6, interferon (INF)γ, IL-3, and granulocyte/macrophage colony-stimulating factor (GM-CSF), and none of these cytokines proved critical for *in vitro* osteoclastogenesis in this culture system, confirming that T-cell-derived OPGL is the crucial mediator. To exclude the possibility that another surface receptor on fixed T cells activates stromal cells for OPGL expression, we used spleen cells from newborn *opgl*$^{-/-}$ mice as a source of haematopoietic precursors and fixed wild-type CD4$^+$ T cells. In this culture, the only source of OPGL is membrane-bound OPGL on the T cells. Wild-type T cells induced the formation of tartrate-resistant acid phosphatase (TRAP)$^+$ osteoclasts from *opgl*$^{-/-}$ progenitor cells, and osteoclastogenesis was inhibited by addition of OPG (Fig. 1d). Osteoclastogenesis was confirmed by detection of the osteoclast-specific markers calcitonin receptor (CTR), RANK (Fig. 1e), cathepsin K (Fig. 1f) and β_3-integrin (Fig. 1g). Thus, T-cell-triggered osteoclasts display a typical osteoclast phenotype (TRAP$^+$, CTR$^+$, cathepsin K$^+$, β_3-integrin$^+$, RANK$^+$). These results provide genetic evidence that activated T cells can directly trigger osteoclastogenesis through membrane-bound and soluble OPGL.

To evaluate whether T-cell activation and expression of OPGL affect bone physiology *in vivo*, we explored the phenotype of *ctla4*$^{-/-}$ mice, in which T cells are spontaneously activated[18]. All *ctla4*$^{-/-}$ mice displayed severe osteoporosis compared with heterozygote littermates (Fig. 2a–d). To further explore the effect of spontaneously activated T cells on bone metabolism, we adoptively transferred *ctla4*$^{+/-}$ or *ctla4*$^{-/-}$ bone marrow cells into lymphocyte-deficient

rag1$^{-/-}$ mice[19] and examined bone structure eight weeks after the cell graft. *rag1*$^{-/-}$ mice have normal numbers of osteoclasts, normal bone morphology and normal bone mineral densities (data not shown). Transfer of *ctla4*$^{-/-}$ cells into *rag1*$^{-/-}$ mice caused a significant decrease in total and trabecular bone mineral densities compared with control *ctla4*$^{+/-}$*rag1*$^{-/-}$ chimaeras and *rag1*$^{-/-}$ mice (Table 1). Histologically, *ctla4*$^{-/-}$*rag1*$^{-/-}$ chimaeric mice exhibited extended resorption of trabecular bone below the growth plates and epiphyses of the femur and tibia (Fig. 2e–h). In addition to decreased mineral density, actual bone loss was observed by histomorphometry (Table 2). Whereas only a few TRAP^{+} osteoclasts were detectable in *ctla4*$^{+/-}$*rag1*$^{-/-}$ mice, osteoclast numbers were significantly increased in *ctla4*$^{-/-}$*rag1*$^{-/-}$ mice (Table 2, and Fig. 2i, j). We observed a similar loss in bone after transfer of purified *ctla4*$^{-/-}$ T cells into *rag1*$^{-/-}$ mice and transfer of purified *ctla4*$^{-/-}$ T cells into *opgl*$^{-/-}$ mice (data not shown), implying that activated T cells can directly cause bone loss *in vivo*. Daily injection of *ctla4*$^{-/-}$ mice with the decoy receptor OPG, which blocks OPGL action, increased bone density and significantly reduced the number of osteoclasts at the growth plates (Table 2, and Fig. 2k, l). These results show that

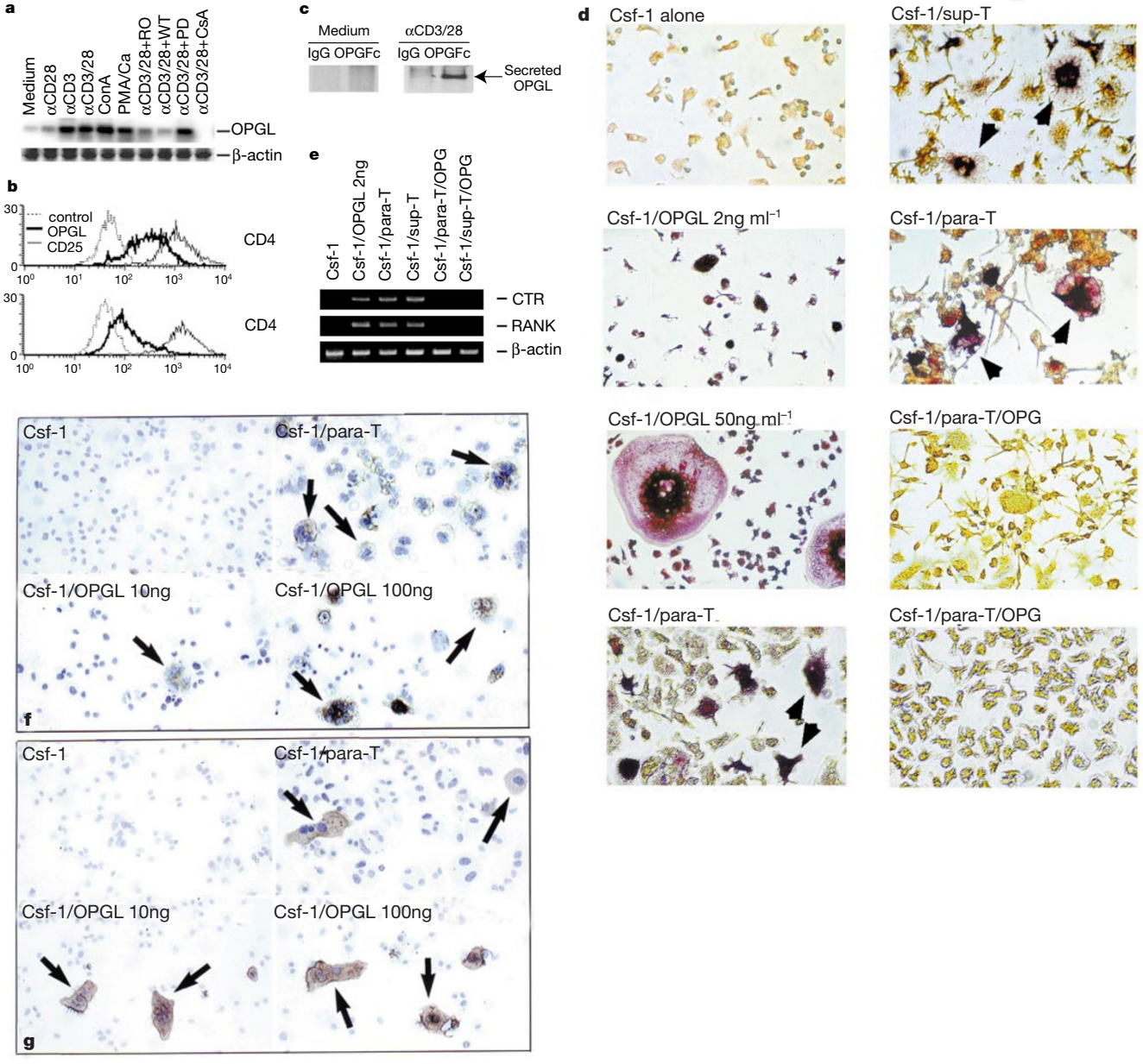

Figure 1 Activated T cells induce osteoclastogenesis through OPGL. **a**, Purified CD4^{+} lymph-node T cells were activated for 16 h with the indicated stimuli in the presence or absence of the signalling inhibitors RO, WT, PD and CsA (see Methods). OPGL and β-actin mRNA expression were detected by RT-PCR. **b**, Expression of OPGL on the surfaces of T cells stimulated with anti-CD3ε plus anti-CD28 antibodies for 4 days. OPGL expression was detected by FACS. CD25 expression is shown to control for activation. **c**, Expression of secreted OPGL protein in supernatants of control T cells (left) or T cells stimulated with anti-CD3 plus anti-CD28 for 2 days (right). **d**, *In vitro* osteoclastogenesis. Bone marrow precursors from wild-type mice (top six panels) and newborn *opgl*$^{-/-}$ mice (bottom two panels) were cultured with Csf-1 alone; Csf-1 plus OPGL; Csf-1 plus supernatant of activated T cells (csf-1/sup-T); Csf-1 plus fixed OPGL^{+}CD4^{+} T cells (csf-1/para-T); or Csf-1 plus fixed OPGL^{+}CD4^{+} T cells plus OPG (500 ng ml^{-1}) (csf-1/para-T/OPG). Arrowheads show TRAP^{+} osteoclasts. **e**–**g**, Calcitonin receptor (CTR), RANK, cathepsin K and β_3-integrin expression. Haematopoietic progenitors from *opgl*$^{-/-}$ mice were cultured as above. CTR, RANK and β-actin mRNA expression were detected by RT-PCR (**e**). Expression of cathepsin K (**f**) and β_3-integrin (**g**) was detected by immunostaining. Arrows indicate osteoclasts.

systemic activation of T cells leads to bone loss *in vivo* through OPGL.

Arthritis in humans is characterized by synovial inflammation, erosion of bone and cartilage, severe joint pain and ultimately life-long crippling[15]. In Lewis rats, experimental induction of adjuvant-induced arthritis (AdA) leads to severe inflammation in the bone marrow and soft tissues surrounding joints accompanied by extensive local bone and cartilage destruction, loss of bone mineral density and crippling[20]. This condition in rats mimics many of the clinical and pathological features of human rheumatoid arthritis. Lesions in AdA are strictly dependent on T-cell activation[21]. Thus, we tested the role of OPGL in the pathogenesis of AdA arthritis in Lewis rats. OPGL protein was expressed on the surface of activated T cells isolated from rats showing clinical onset of arthritis, and OPGL mRNA could be detected in both synovial cells and inflammatory cells by *in situ* hybridization. At the onset of disease, arthritic rats were either left untreated or treated with OPG for seven days. Inhibition of OPGL through OPG had no effect on the severity of inflammation (Fig. 3a); however, OPG treatment completely abolished the loss of mineral bone density (Fig. 3b). Histologically, OPG-treated arthritic rats exhibited minimal loss of cortical and trabecular bone, whereas untreated AdA animals developed severe bone lesions characterized by partial to complete destruction of cortical and trabecular bone, erosion of the articular cartilages and clinical crippling (Fig. 4a–f). Bone destruction in untreated arthritic rats correlated with a dramatic increase in osteoclast numbers, whereas OPG treatment prevented the accumulation of osteoclasts (Figs 3c and 4e, f). These results show that OPGL is a key mediator of joint destruction and bone loss in adjuvant arthritis.

Alteration of cartilage structures leading to cartilage collapse constitutes a critical step in arthritic joint destruction. There is controversy about whether cartilage destruction occurs independently of bone loss, or whether damage to the subchondral bone indirectly causes cartilage deterioration[22,23]. Because OPG treatment prevented bone loss but not inflammation, we analysed the structural integrity of joint cartilage. In untreated arthritic rats, partial or complete erosion of the cartilage matrix in both the central and peripheral regions of joint surfaces was observed, as assessed by loss of toluidine blue staining (Fig. 4h). These erosions occurred in association with destruction of the underlying bony plate. In striking contrast, the integrity of cartilage was preserved in OPG-treated arthritic rats (Fig. 4i). Whether OPG protects the cartilage

Table 2 Numbers of osteoclasts in the cortical bone

Groups	Number of osteoclasts in bone area	Number of osteoclasts in total area	BA%TA
ctla4$^{+/-}$	7.69 ± 2.30	1.82 ± 0.73	23.5 ± 3.4
ctla4$^{-/-}$	77.69 ± 23.12*	11.63 ± 3.85*	14.4 ± 1.7*
ctla4$^{-/-}$/*OPG*	33.52 ± 12.18†	4.00 ± 1.37†	ND
rag1$^{-/-}$	6.86 ± 3.43	2.58 ± 1.33	35.9 ± 5.6
ctla4$^{+/-}$*rag1*$^{-/-}$	18.81 ± 13.12	7.74 ± 6.09	33.7 ± 5.4
ctla4$^{-/-}$*rag1*$^{-/-}$	167.06 ± 32.59‡	26.43 ± 1.80‡	16.6 ± 1.7‡

Osteoclast numbers (mean ± s.e.m.; see Methods) were counted in tibial bones from *ctla4*$^{+/-}$ ($n = 3$), *ctla4*$^{-/-}$ ($n = 3$) and *ctla4*$^{-/-}$ mice injected subcutaneously daily with OPG (1 mg kg^{-1} body weight in PBS) on days 21–29 after birth; and *rag1*$^{-/-}$ ($n = 3$) and *rag1*$^{-/-}$ mice reconstituted with *ctla4*$^{+/-}$ ($n = 3$) or *ctla4*$^{-/-}$ ($n = 3$) bone marrow cells eight weeks after cell transfer. Histomorphometry was performed on cortical bone in the diaphysis of tibial bones and is shown as mean ± s.d. of bone area (BA) as a percentage of total tissue area (TA). ND, not determined.
* Statistically significant differences between *ctla4*$^{+/-}$ and *ctla4*$^{-/-}$ groups.
† Statistically significant differences between *ctla4*$^{-/-}$ and OPG-treated *ctla4*$^{-/-}$ groups.
‡ Statistically significant differences between *ctla4*$^{+/-}$*rag1*$^{-/-}$ and *ctla4*$^{-/-}$*rag1*$^{-/-}$ groups (Student's *t*-test; $P < 0.05$).

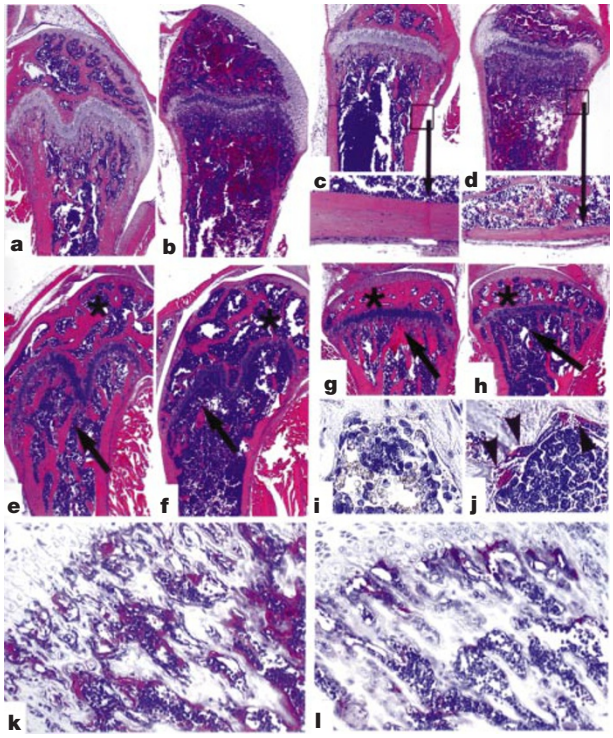

Figure 2 Activated T cells affect bone physiology *in vivo*. **a**–**d**, Histology of femur (**a**, **b**) and tibia (**c**, **d**) of *ctla4*$^{+/-}$ (**a**, **c**) and *ctla4*$^{-/-}$ (**b**, **d**) mice. Note significantly reduced thickness of cortical bone in *ctla4*$^{-/-}$ mice. **e**–**h**, Histology of femur (**e**, **f**) and tibia (**g**, **h**) from *rag1*$^{-/-}$ mice reconstituted with *ctla4*$^{+/-}$ (**e**, **g**) and *ctla4*$^{-/-}$ (**f**, **h**) bone marrow cells. Samples were analysed eight weeks after cell transfer. *ctla4*$^{-/-}$*rag1*$^{-/-}$ mice show extended resorption of trabecular bone below the growth plate (arrows) and in the epiphysis (asterix) of both femur and tibia. **i**, **j**, Increased number of TRAP^{+} osteoclasts in *ctla4*$^{-/-}$*rag1*$^{-/-}$ (**j**) compared with *ctla4*$^{+/-}$*rag1*$^{-/-}$ chimaeras (**i**). **k**, **l**, OPG treatment reduces osteoclast numbers in *ctla4*$^{-/-}$ mice. *ctla4*$^{-/-}$ mice were injected subcutaneously daily with PBS (**k**) or OPG (1 mg kg^{-1} body weight in PBS) (**l**) on days 21–29 after birth. Note the decreased number of TRAP^{+} osteoclasts in the femur growth plate of OPG-treated *ctla4*$^{-/-}$ mice (**l**) (TRAP, 20×). Staining: HE (**a**–**h**); TRAP (**i**–**l**).

indirectly by maintain the underlying subchondral bone or has a direct role in cartilage maintenance needs to be determined. In addition, we have found that T cells isolated from joints of all human rheumatoid arthritis ($n = 20$) and all osteoarthritis ($n = 10$) patients express OPGL (see Supplementary Information). The significance of T cell-derived OPGL in human arthritis needs to be determined. These data show that OPGL is a key regulator of bone metabolism, and that inhibition of OPGL activity by OPG can prevent cartilage destruction, a critical, irreversible step in the pathogenesis of arthritis.

Our results show that activated T cells can regulate systemic and local bone loss through OPGL. In summary, activated T cells produce OPGL and can directly trigger osteoclastogenesis *in vitro*; activated T cells from *ctla4*$^{-/-}$ mice have a destructive effect on bone mineral density *in vivo* that can be reversed through inhibition of OPGL; and inhibition of OPGL through OPG can completely prevent bone and cartilage loss in a T-cell-dependent arthritis model. In addition, we have found that six out of seven spontaneously arising T-cell lymphomas in mice express high levels of OPGL on T-cell surfaces, and that these lymphoma cells can directly support *in vitro* osteoclastogenesis (data not shown). As mutant mice lacking T and B cells exhibit normal bone morphology and bone mineral densities, T cells are probably not required for normal

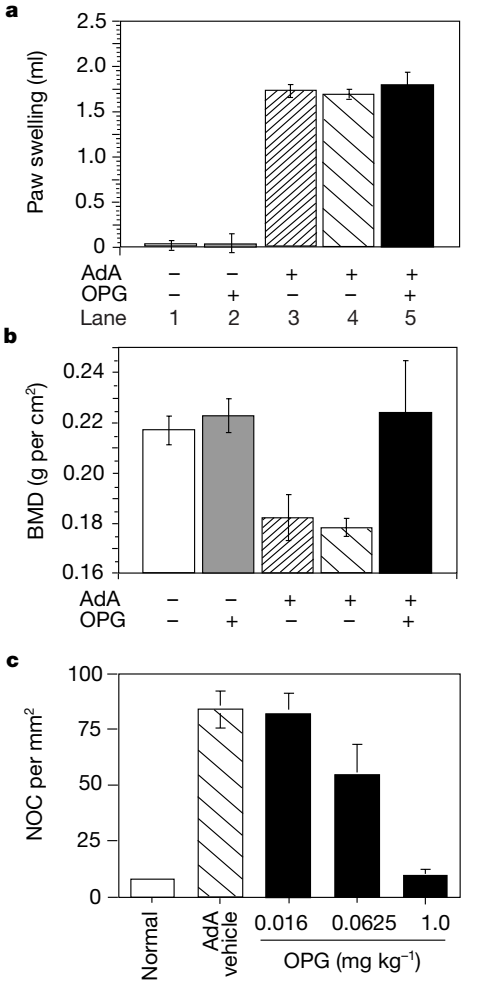

Figure 3 OPG blocks bone loss in adjuvant-induced arthritis (AdA). **a**, Severity of inflammation was calculated by measuring the volume of hind paw swelling on day 16 after initiation of disease. Lane 1, untreated controls; lane 2, OPG (1 mg kg^{-1} day^{-1}) treatment but no AdA; lane 3, AdA but no OPG treatment; lane 4, AdA plus OPG vehicle control; lane 5, AdA plus OPG (1 mg kg^{-1} day^{-1}). Mean values of swelling (water displacement (ml)) ±s.d. are shown ($n = 6$ per group). Paw swelling was similar between AdA and AdA plus OPG groups at all time points (days 9–15). **b**, Bone mineral density (BMD) of the tibiotarsal region was determined on day 16. Lanes are as in (**a**). Mean values of BMD ± s.d. are shown ($n = 6$ per group). **c**, Numbers of osteoclasts (NOC) per mm^2 of total bone area in the navicular tarsal bone were determined on day 16. For induction of AdA in Lewis rats and daily subcutaneous injections with soluble OPG from day 9 (onset of disease) to day 15, see Methods.

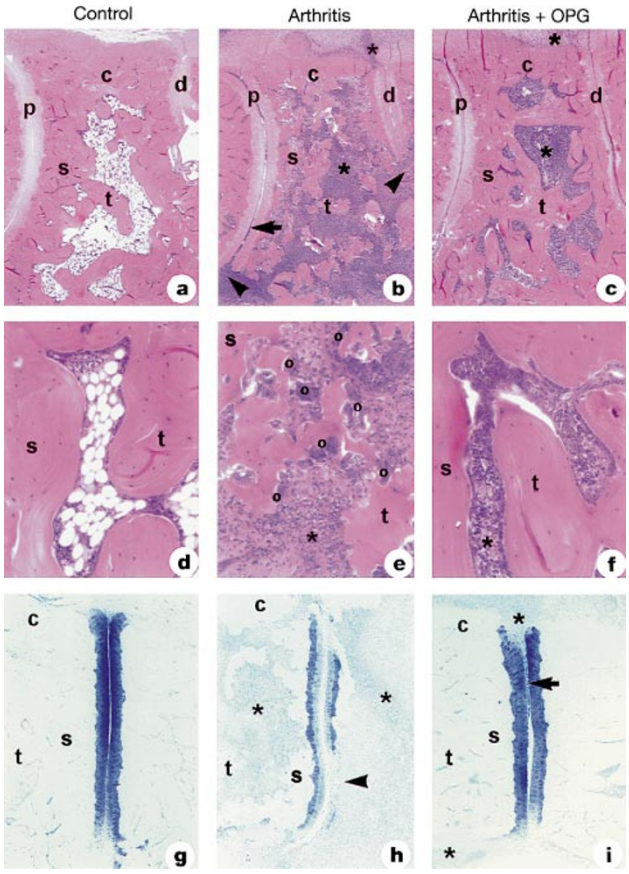

Figure 4 OPG prevents bone and cartilage destruction even in the presence of severe inflammation. **a**, **d**, Bone and joint structure in the normal hind paw showing dense bony plates, intact articular cartilages and marrow cavities containing scattered haematopoietic precursor cells. Proximal (p) distal (d) intertarsal joints. **b**, **e**, Disrupted bone and joint structure in AdA rats (day 16) with severe mononuclear infiltration in the bone marrow (asterisk), and pannus (arrow); advanced destruction (arrowheads) of cortical (c), subchondral (s) and trabecular (t) bone; and erosion of the articular cartilages. The marrow cavity contains a marked mononuclear cell infiltration (asterisk) containing numerous osteoclasts (o). These rats show severe clinical crippling. **c**, **f**, Preserved bone and joint structure of AdA rats (day 16) treated with OPG (1 mg kg^{-1} day^{-1}) on days 9–15. OPG-treated rats exhibit extensive mononuclear cell infiltration of bone marrow (asterisk) and pannus formation (arrow), but cortical (c), subchondral (s) and trabecular (t) bone and articular cartilages are intact. Note the absence of osteoclasts as compared with non-OPG-treated rats (**e**). These rats do not show any clinical signs of crippling. **g**, Normal cartilage integrity in control rats as determined by toluidine blue staining. The matrix of normal articular cartilage is uniformly stained, and the underlying bony plates are dense. **h**, Cartilage matrix degeneration in AdA rats (day 16). Uniform pallor (small arrow) in the upper half of articular cartilages denotes extensive loss of matrix proteoglycans. Subchondral (s), cortical (c) and trabecular (t) bone is extensively eroded, and the marrow cavity is filled with inflammatory cells (asterisks). **i**, OPG treatment preserves matrix proteoglycans of arthritic rats (day 16) treated with OPG (1 mg kg^{-1} day^{-1}) on days 9–15. Note modest reduction of toluidine blue staining in peripheral cartilage regions that are in direct contact with inflamed synovial tissue (asterisks) or pannus (arrows). Subchondral (s), cortical (c) and trabecular (t) bone is intact. Staining: HE (**a**–**f**); toluidine blue (**g**–**i**). Magnifications: 50× (**a**–**c**); 250× (**d**–**f**); 75× (**g**–**i**).

bone homeostasis. Local inflammation within the bone due to metastasis, infections or fractures, or joint inflammation in arthritis, however, attracts T cells which appear to actively participate in bone remodelling through production of OPGL. To our knowledge, our results provide the first definitive linkage between activated T cells and bone homeostasis and that systemic or local activation of T cells triggers bone loss through expression of OPGL. These findings provide the molecular explanation for bone loss associated with diseases having immune-system involvement, such as adult and childhood leukaemias, autoimmunity and various viral infections such as hepatitis and HIV. Thus, inhibition of OPGL function might ameliorate many osteopenic conditions and prevent the bone destruction and cartilage damage that ultimately cause crippling in arthritis. □

Methods

T-cell activation and osteoclastogenesis

Purified (>98% $CD3^+$) $CD8^+$ and $CD4^+$ T cells (10^6 per well) were seeded in Iscove's modified Dulbecco medium (IMDM) and stimulated with anti-CD3ε (2 μg ml^{-1}) and anti-CD28 (200 ng ml^{-1}) antibodies (PharMingen) in the absence or presence of the MAPK/ERK inhibitor PD98059 (PD, 4 μM), the calcineurin inhibitor cyclosporin A (CsA, 100 ng ml^{-1}), the PKC inhibitor RO-31-8220 (RO, 2 μM) or the P13K inhibitor wortmannin (WT, 2 μM) for various times. OPGL mRNA expression was detected by RT-PCR as described[17]. Membrane-bound OPGL was detected by double staining using OPG-fluorescein isothiocyanate (FITC) and anti-CD4-PE or anti-CD8-PE. For CD25 (IL-2Rα chain) expression, cells were stained with anti-CD25-FITC and anti-CD4-PE or anti-CD8-PE. Viable cells were collected by FACS analysis. For detection of secreted OPGL protein, T cells (5×10^5) were stimulated with anti-CD3ε (2 μg ml^{-1}) plus anti-CD28 (200 ng ml^{-1}) for 2 days and metabolically labelled with 1 μCi ml^{-1} of [^{35}S]methionine for the last 100 min of incubation. Labelled OPGL was immunoprecipitated from supernatants using either 1 μg ml^{-1} of human OPG-Fc[1] or 1 μg of isotype-matched control IgG. In addition, secreted OPGL protein was determined in supernatants of anti-CD3ε and anti-CD28 stimulated T cells (4 days) by ELISA. OPGL expression on the surface of T cells was detectable 2 days after stimulation with anti-CD3 and anti-CD28, and maximum expression was observed at day 4 of stimulation. Throughout the whole time of the co-culture, expression of OPGL on fixed T cells was stable (data not shown). For *in vitro* osteoclastogenesis, purified $CD4^+$ T cells were stimulated for 4 days with anti-CD3ε plus anti-CD28 and fixed with 2.5% paraformaldehyde. Fixed T cells (10^6 cells per well) were co-cultured with non-adherent hematopoietic progenitors (10^5 cells well^{-1}) from bone marrow cells of wild-type mice or spleen cells of newborn *opgl*$^{-/-}$ mice in the presence of 30 ng ml^{-1} colony-stimulating factor-1 (Csf-1; Genzyme) in a flat-bottom 96-well plate. The soluble decoy receptor OPG (500 ng ml^{-1}) was added to control co-cultures to confirm that the observed effects were mediated by OPGL. OPG was used as described[1]. Osteoclast differentiation was evaluated on day 4 by cytochemical staining for TRAP, which specifically labels osteoclasts with a red dye, immunohistochemistry to detect Cathepsin K and β_3-integrin, and by RT-PCR for calcitonin receptor (CTR) and RANK expression. PCR primers were β-actin sense; CACTGCCGCATCCTCTTCCTC; β-actin antisense, GCTGTCGCCTTCACCGTTCCA; calcitonin receptor sense, ACAACTGCTGG CTGAGTG; calcitonin receptor antisense, GAAGCAGTAGATAGTCGCCAC; RANK sense, GCAACCTCCAGTCAGCA; RANK antisense, GAAGTCACAGCCCTCAGAATC. To detect expression of β_3-integrin and cathepsin K protein, *opgl*$^{-/-}$ spleen cells were cultured with wild-type T cells for 4 days, and the expression was detected as described[24].

In vivo bone remodelling

ctla4$^{-/-}$ and *rag1*$^{-/-}$ gene-targeted mice were back-crossed onto a C57BL/6 background for at least eight generations[18,19]. For chimaeras, bone marrow cells or purified lymph-node T cells from *ctla4*$^{+/-}$ and *ctla4*$^{-/-}$ littermate mice were transferred into 6-week-old irradiated (300 rad) *rag1*$^{-/-}$ and into 6-week-old irradiated (500 rad) *opgl*$^{-/-}$ mice. Chimaerism was monitored by FACS staining for labelled monoclonal antibodies reactive to surface markers on T cells (anti-CD4, anti-CD8, anti-TCR) or B cells (anti-CD19, anti-B220, anti-sIgM) (all from PharMingen). In all experiments, chimaerism of these mice was more than 90%. RAG-chimaeric mice were necropsied 8–10 weeks after cell transfer. *ctla4*$^{-/-}$ T cell → *opgl*$^{-/-}$ chimaeras were necropsied 12 days after cell transfer. Bone mineral density was determined as described[2]. Histology and histomorphometry were done as described[2]. Osteoclast numbers were determined in a 0.5 × 1.0 mm rectangle area distal to the growth plate in the tibia. The field of measurement started adjacent to the growth plate, in the centre of the marrow cavity not including the cartilage or cortical bone.

Adjuvant-induced arthritis (AdA)

Eight- to nine-week male Lewis rats were given subcutaneous (s.c.) injections of *Mycobacterium tuberculosis* (0.5 mg emulsified in 50 μl of paraffin oil) into the base of the tail (Difco Laboratories, Detroit). At the onset of clinical inflammation (day 9 after inoculation), animals were injected s.c. with soluble OPG (0.016, 0.0625 and 1 mg kg^{-1} day^{-1})[1] on each of days 9–15. On day 16, animals were killed and bone mineral density (BMD) of the tibiotarsal region was determined by DexaScan of the hind paws using a dual-energy X-ray absorptiometer (Hologic QDR 4500). Severity of inflammation was monitored daily on days 8–16 by measuring the volume of hind paws by water displacement. Paws were processed into paraffin as described above, and serial sections were stained with haematoxylin and eosin (HE) (to grade inflammatory and bone destructive changes) and toluidine blue (to assess the integrity of cartilage by visualizing matrix proteoglycans). Criteria for scoring the extent of inflammation and cartilage matrix integrity have been defined[20]. Numbers of osteoclasts were counted in the navicular tarsal bone using histomorphometric measurements by tracing the section image onto a digitizing plate with the aid of a camera lucida and 'Osteomeasure' (Osteometrics Inc., Decatur, GA) bone analysis software. Two separate 560 × 560 μm regions of the talus bone were measured for each individual section. Osteoclasts included in the measurement were identified morphologically and had to be in contact with a bone surface. Experimental results are reported as the average number of osteoclasts (NOC) per mm^2 tissue of both left and right ankles. Animal experiments were in accordance with institutional guidelines.

Received 6 August; accepted 23 September 1999.

1. Simonet, W. S. *et al.* Osteoprotegerin: a novel secreted protein involved in the regulation of bone density. *Cell* **89,** 309–319 (1997).
2. Lacey, D. L. *et al.* Osteoprotegerin ligand is a cytokine that regulates osteoclast differentiation and activation. *Cell* **93,** 165–176 (1998).
3. Kong, Y. Y. *et al.* OPGL is a key regulator of osteoclastogenesis, lymphocyte development and lymph-node organogenesis. *Nature* **397,** 315–323 (1999).
4. Anderson, D. M. *et al.* A homologue of the TNF receptor and its ligand enhance T-cell growth and dendritic-cell fucntion. *Nature* **390,** 175–179 (1997).
5. Wong, B. r. *et al.* TRANCE (tumor necrosis factor [TNF]-related activation-induced cytokine), a new TNF family member predominantly expressed in T cells, is a dendritic cell-specific survival factor. *J. Exp. Med.* **186,** 2075–2080 (1997).
6. Hsu, H. *et al.* Tumor necrosis factor receptor family member RANK mediates osteoclast differentiation and activation induced by osteoprotegerin ligand. *Proc. Natl Acad. Sci. USA* **96,** 3540–3545 (1999).
7. Wong, B. R. *et al.* TRANCE is a novel ligand of the tumor necrosis factor receptor family that activates c-Jun N-terminal kinase in T cells. *J. Biol. Chem.* **272,** 25190–25194 (1997).
8. Felix, R., Hofstetter, W. & Cecchini, M. G. Recent developments in the understanding of the pathophysiology of osteopetrosis. *Eur. J. Endocrinol.* **134,** 143–156 (1996).
9. Roodman, G. D. Advances in bone biology: the osteoclast. *Endocr. Rev.* **17,** 308–332 (1996).
10. Roodman, G. D. Paget's disease and osteoclast biology. *Bone* **19,** 209–212 (1996).
11. Coleman, R. E., Smith, P. & Rubens, R. D. Clinical course and prognostic factors following bone recurrence from breast cancer. *Br. J. Cancer* **77,** 336–340 (1998).
12. Stellon, A. J., Davies, A., Compston, J. & Williams, R. Bone loss in autoimmune chronic active hepatitis on maintenance corticosteroid therapy. *Gastroenterology* **89,** 1078–1083 (1985).
13. Oliveri, M. B., Mautalen, C. A., Rodriguez Fuchs, C. A. & Romanelli, M. C. Vertebral compression fractures at the onset of acute lymphoblastic leukemia in a child. *Henry Ford Hosp. Med. J.* **39,** 45–48 (1991).
14. Piepkorn, B. *et al.* Bone mineral density and bone metabolism in diabetes mellitus. *Horm. Metab. Res.* **29,** 584–591 (1997).
15. Feldmann, M., Brennan, F. M. & Maini, R. N. Role of cytokines in rheumatoid arthritis. *Annu. Rev. Immunol.* **14,** 397–440 (1996).
16. Kotake, S. *et al.* IL-17 in synovial fluids from patients with rheumatoid arthritis is a potent stimulator of osteoclastogenesis. *J. Clin. Invest.* **103,** 1345–1352 (1999).
17. Josien, R., Wong, B. R., Li, H. L., Steinman, R. M. & Choi, Y. TRANCE, a TNF family member, is differentially expressed on T cell subsets and induces cytokine production in dendritic cells. *J. Immunol.* **162,** 2562–2568 (1999).
18. Waterhouse, P. *et al.* Lymphoproliferative disorders with early lethality in mice deficient in Ctla-4. *Science* **270,** 985–988 (1995).
19. Mombaerts, P. *et al.* RAG-1-deficient mice have no mature B and T lymphocytes. *Cell* **68,** 869–877 (1992).
20. Bendele, A. *et al.* Efficacy of sustained blood levels of interleukin-1 receptor antagonist in animal models of arthritis: comparison of efficacy in animal models with human clinical data. *Arthritis Rheum.* **42,** 498–506 (1999).
21. Panayi, G. S., Lanchbury, J. S. & Kingsley, G. H. The importance of the T cell in initiating and maintaining the chronic synovitis of rheumatoid arthritis. *Arthritis Rheum.* **35,** 729–735 (1992).
22. Muller-Ladner, U., Gay, R. E. & Gay, S. Molecular biology of cartilage and bone destruction. *Curr. Opin. Rheumatol.* **10,** 212–219 (1998).
23. Conway, J. G. *et al.* Inhibition of cartilage and bone destruction in adjuvant arthritis in the rat by a matrix metalloproteinase inhibitor. *J. Exp. Med.* **182,** 449–457 (1995).
24. Faust, J. *et al.* Osteoclast markers accumulate on cells developing from human peripheral blood mononuclear precursors. *J. Cell. Biochem.* **72,** 67–80 (1999).

Supplementary information is available on *Nature*'s World-Wide Web site (http://www.nature.com) or as paper copy from the London editorial office of *Nature*.

Acknowledgements

We thank E. C. Keystone for providing patient samples and C. Dunstan for critical comments. Technical assistance was provided by Y. Cheng, E. Julian, C. Burgh, A. Shahinian and D. Duryea. We are grateful to M. E. Saunders for scientific editing and A. Hessel, A. Oliveira dos Santos, K. Bachmaier, T. Sasaki and all other members of the laboratory for comments.

Correspondence and requests for materials should be addressed to J.M.P. (e-mail: jpenning@amgen.com).